Dynamics of oscillating magnetized relativistic tori around a Schwarzschild black hole

P J Montero[1], J A Font[1], L Rezzolla[2,3] and O Zanotti[4]

[1] Departamento de Astronomía y Astrofísica, Universidad de Valencia, Valencia, Spain
[2] Max-Planck-Institut für Gravitationsphysik, Albert-Einstein-Institut, Potsdam, Germany
[3] Department of Physics, Louisiana State University, Baton Rouge, USA
[4] Dipartimento di Astronomia e Scienza dello Spazio, Universita di Firenze, Firenze, Italy

E-mail: pedro.montero@uv.es

Abstract. We present a comprehensive numerical study of the dynamics of magnetized relativistic axisymmetric tori orbiting in the background spacetime of a Schwarzschild black hole. The tori are modeled as having a purely toroidal magnetic field and a constant distribution of the specific angular momentum. Following previous investigations of tori in a purely hydrodynamical context, the dynamics of these objects has been studied upon the introduction of a perturbation which, for the values of the magnetic field considered here, triggers quasi-periodic oscillations (QPOs) lasting tens of orbital periods. As in the hydrodynamical case, the spectral distribution of the eigenfrequencies shows the presence of a fundamental p-mode and of overtones in a harmonic ratio: $2 : 3 : \ldots$. We comment on the implications of these results on the phenomenology observed for the QPOs in low-mass X-ray binaries containing a black hole candidate.

1. Introduction

Magnetic fields are thought to play an important role on the dynamics of accretion discs orbiting around black holes. They can be the source of viscous processes within the disc and of the so called magnetorotational instability (MRI) (Balbus & Hawley [1]) that self-regulates the accretion process by transferring angular momentum outwards. In addition to this, the development and collimation of strong relativistic outflows or jets is closely related to the presence of magnetic fields (Blandford & Znajek [2]).

General relativistic magnetohydrodynamic (GRMHD) numerical simulations are probably the most accurate approach for the investigation of the dynamics of relativistic, magnetized accretion discs. Recently, there has been a major step forward in the modeling of such systems, implementation of the GRMHD equations in numerical codes developed by a number of groups (De Villiers & Hawley [3]; Gammie et al. [4]; Antón et al. [5]) that have been applied to the investigation of the MRI in accretion discs. Moreover, Komissarov [6] has derived an analytic solution for an axisymmetric and stationary torus with a toroidal magnetic field which may be used as a code test or as initial data for studies of the dynamics of tori with a toroidal magnetic field.

In a purely hydrodynamical context, Zanotti et al. [7] found through fully nonlinear hydrodynamic numerical simulations that relativistic tori may undergo a persistent phase of oscillations when subject to perturbations. Here, we aim to investigate further this type of mode of oscillation of accretion tori by taking into account the effect of a toroidal magnetic field. Thus, we present a study of the axisymmetric p-mode oscillations of tori with a toroidal magnetic field and its implications on the high-frequency

quasi-periodic oscillations (HFQPOs) observed in low-mass X-ray binaries (LMXBs) with a black hole candidate.

The paper is organized as follows: In Section 2 we briefly review the mathematical framework we use for the implementation of the GRMHD equations in our numerical code. Next, in Section 3, we present the initial models, while in Section 4, we describe the techniques for the numerical solution of the GRMHD equations. Section 5, contains the discussion of the results, and finally, Section 6 is devoted to the conclusions. Throughout the paper we use geometrized units with $G = c = 1$. Greek indeces run from 0 to 3 and Latin indeces from 1 to 3.

2. Mathematical framework

The nonlinear, axisymmetric, GRMHD code used to carry out the simulations we report solves numerically the GRMHD equations within the framework of the 3+1 formalism as presented by Antón et al. [5]. We write the evolution equations for the matter fields and the induction equation for the evolution of the magnetic field as measured by an Eulerian observer in a conservative form. Writing the system of evolution equations in this form allows us to exploit their hyperbolic character and to make use of high resolution shock capturing (HRSC) methods.

Following the procedure laid out in Antón et al. [5], the GRMHD equations are cast in flux-conservative hyperbolic form:

$$\frac{1}{\sqrt{-g}}\left(\frac{\partial\sqrt{\gamma}\mathbf{F}^0}{\partial x^0}+\frac{\partial\sqrt{-g}\mathbf{F}^i}{\partial x^i}\right)=\mathbf{S}, \tag{1}$$

where $\mathbf{F}^0$ represents the state vector given by

$$\mathbf{F}^0 \;=\; \begin{bmatrix} D \\ S_j \\ \tau \\ B^k \end{bmatrix}, \tag{2}$$

and we have used the following definitions

$$D = \rho W, \tag{3}$$
$$S_j = \rho(h+b^2/\rho)W^2 v_j - \alpha b^0 b_j, \tag{4}$$
$$\tau = \rho(h+b^2/\rho)W^2 - (p+b^2/2) - \alpha^2(b^0)^2 - D, \tag{5}$$

where ρ is the rest-mass density of the fluid, W is the Lorentz factor, h is the specific enthalpy of the fluid, p the isotropic pressure, v_i the components of the spatial velocity, α is the lapse function, and the four components of the magnetic field in the comoving frame are given by b^μ. Correspondingly, the fluxes $\mathbf{F}^i$ are given by

$$\mathbf{F}^i \;=\; \begin{bmatrix} D\tilde{v}^i \\ S_j\tilde{v}^i + (p+b^2/2)\delta^i_j - b_j B^i/W \\ \tau\tilde{v}^i + (p+b^2/2)v^i - \alpha b^0 B^i/W \\ \tilde{v}^i B^k - \tilde{v}^k B^i \end{bmatrix}, \tag{6}$$

with $\tilde{v}^i = v^i - \frac{\beta^i}{\alpha}$, β^i being the shift vector, and the corresponding source terms $\mathbf{S}$ are given by

$$\mathbf{S} \;=\; \begin{bmatrix} 0 \\ T^{\mu\nu}\left(\frac{\partial g_{\nu j}}{\partial x^\mu} - \Gamma^\delta_{\nu\mu} g_{\delta j}\right) \\ \alpha\left(T^{\mu 0}\frac{\partial \ln\alpha}{\partial x^\mu} - T^{\mu\nu}\Gamma^0_{\nu\mu}\right) \\ 0^k \end{bmatrix}, \tag{7}$$

where $0^k \equiv (0,0,0)^T$, and $T^{\mu\nu}$ and $\Gamma^{\mu}_{\nu\delta}$ are the stress-energy tensor and the Christoffel symbols respectively. Note that the following fundamental relations hold between the four components of the magnetic field in the comoving frame, b^μ, and the three vector components B^i measured by the Eulerian observer associated to the 3+1 splitting of the metric:

$$b^0 = \frac{WB^i v_i}{\alpha}, \tag{8}$$

$$b^i = \frac{B^i + \alpha b^0 u^i}{W}\,. \tag{9}$$

Finally, the modulus of the magnetic field can be written as

$$b^2 = \frac{B^2 + \alpha^2 (b^0)^2}{W^2}\,, \tag{10}$$

where $B^2 = B^i B_i$.

3. Stationary and axisymmetric fluid configurations with a toroidal magnetic field

The initial magneto-fluid configuration we use is an extension of the stationary solution of a thick disc orbiting around a black hole described by Kozlowski et al. [8], Abramowicz et al. [9] and more recently by Font & Daigne [10]. This new solution of a magnetized relativistic torus has been recently proposed by Komissarov [6], where the basic equations that are solved to construct the initial models in equilibrium are the continuity equation $\nabla_\mu(\rho u^\mu) = 0$, the conservation of energy-momentum $\nabla_\mu T^{\mu\nu} = 0$ and Maxwell's equation $\nabla_\mu({}^*F^{\mu\nu}) = 0$ where the symbol ∇_μ refers to the covariant derivative with respect to the four-metric and ${}^*F^{\mu\nu}$ is the dual of the Faraday tensor defined as ${}^*F^{\mu\nu} = u^\mu b^\nu - u^\nu b^\mu$, u^μ being the fluid four-velocity. As usual in ideal relativistic MHD the stress-energy tensor $T^{\mu\nu}$ is expressed as

$$T^{\mu\nu} \equiv (\rho h + b^2) u^\mu u^\nu + \left(p + \frac{b^2}{2}\right) g^{\mu\nu} - b^\mu b^\nu, \tag{11}$$

where $g^{\mu\nu}$ is the metric tensor.

We solve the equilibrium equations and build stationary and axisymmetric fluid configurations with a toroidal magnetic field orbiting around a Schwarzschild black hole and obeying a constant distribution of the specific angular momentum in the equatorial plane. The difference of the solution we use with that of Komissarov [6] is that we employ a polytropic equation of state of the form $p = \kappa\rho^\gamma$ for the fluid, where κ is the polytropic constant and γ is the adiabatic index, instead of $p = K\omega^q$, where ω is the fluid enthalpy, and K and q are constants . The magnetized relativistic tori fill their outermost closed equipotential surface and thus their inner radii coincide with the position of the cusp, i.e. $r_{\rm in} = r_{\rm cusp}$. The various models differ in the strength of the toroidal magnetic field which is parametrized by the ratio of the magnetic-to-gas pressure (β_c) at the centre of the disc. All models are built with an adiabatic index $\gamma = 4/3$ and the polytropic constant κ is fixed such that the ratio $M_{\rm t}/M$ of the torus-to-black hole mass is approximately 0.1. Since the mass of the torus is at most a 10% of that of the black hole we can neglect the effect of the self gravity of the torus which renders justifiable our assumption of studying the disc dynamics in a fixed background spacetime. Moreover, this disc-to-hole mass ratio is in agreement with the outcomes from existing simulations of binary neutron star merger (e.g., Shibata et al. [11,12]).

As we are interested in the study of the oscillation properties of magnetized tori we perturb the models reported in Table 1 by adding a small radial velocity to the initial conditions. This perturbation is parametrized in terms of a dimensionless coefficient η expressing the fraction of the radial velocity to that of the spherically symmetric accretion flow onto a Schwarzschild black hole (Michel [13]), i.e. $v_r = \eta(v_r)_{\rm sph}$.

Table 1. From left to right the columns report the name of the model, the spin of the black hole, the torus-to-hole mass ratio, the specific angular momentum, the adiabatic index, the polytropic constant, the inner and outer radius of the torus, the orbital period at the point of maximum rest-mass density, the maximum rest-mass density and the magnetic-to-gas pressure at the maximum of the rest-mass density.

Model	a	$M_{\rm t}/M$	ℓ_0	γ (cgs)	κ (cgs)	$r_{\rm in}$	$r_{\rm out}$	$t_{\rm orb}$ (ms)	$\rho_{\rm max}$ (cgs)	(β_c)
A1.1	0.0	0.1	3.8	4/3	9.33×10^{13}	4.57	15.88	1.86	1.25×10^{13}	0.00
A1.2	0.0	0.1	3.8	4/3	9.21×10^{13}	4.57	15.88	1.86	1.26×10^{13}	0.01
A1.3	0.0	0.1	3.8	4/3	9.10×10^{13}	4.57	15.88	1.86	1.27×10^{13}	0.02
A1.4	0.0	0.1	3.8	4/3	8.90×10^{13}	4.57	15.88	1.86	1.28×10^{13}	0.04
A1.5	0.0	0.1	3.8	4/3	8.40×10^{13}	4.57	15.88	1.86	1.29×10^{13}	0.1
A1.6	0.0	0.1	3.8	4/3	7.60×10^{13}	4.57	15.88	1.86	1.34×10^{13}	0.2
A1.7	0.0	0.1	3.8	4/3	6.00×10^{13}	4.57	15.88	1.86	1.39×10^{13}	0.5
A1.8	0.0	0.1	3.8	4/3	4.49×10^{13}	4.57	15.88	1.86	1.40×10^{13}	1.0

4. Numerical solution

The system of GRMHD equations, Eq.(1), is solved using a HRSC scheme based on the HLLE solver, except for the induction equation for which we use the constraint transport method designed by Evans & Hawley [14] and Ryu et al. [15]. Second-order accuracy in both space and time is achieved by adopting a piecewise-linear cell reconstruction procedure and a second order, conservative Runge-Kutta scheme, respectively.

The computational grid consists of $N_r \times N_\theta$ zones in the radial and angular directions, respectively. The innermost zone of the radial grid is placed at $r_{\rm min} = r_{\rm horizon} + 0.1 r_g$, where r_g is the gravitational radius of the black hole and the outer boundary in the radial direction is at a distance about 30% larger than the outer radius of the torus, $r_{\rm out}$. The radial grid is built by joining smoothly a first patch which extends from $r_{\rm min}$ to the outer radius of the torus and is logarithmically spaced (with a maximum radial resolution at the innermost grid zone, $\Delta r = 1 \times 10^{-3}$) and a second patch with a uniform grid and which extends up to $r_{\rm max}$. Typically, we use $N_r \simeq 300$. On the other hand, the angular grid consists of $N_\theta = 100$ equally spaced zones and covers the domain from 0 to π. As we cannot handle vacuum regions with our finite difference GRMHD code we introduce a low density "atmosphere" in those parts of the numerical domain not occupied by the torus. We use the spherically symmetric accreting solution described by Michel [13] with its maximum density being $5-6$ orders of magnitude smaller than the maximum rest-mass density of the torus.

5. Results

5.1. Dynamics of magnetized tori in a Schwarzschild background

We have first investigated equilibrium configurations of magnetized tori by performing numerical evolutions of the unperturbed tori and checking the stationarity of the solution for the whole length of the simulations. The dashed line in the left panel of Fig. 1 displays the evolution of the rest-mass density of the unperturbed and weakly magnetized model A1.2. The evolution of the central rest-mass density shows that after a short initial transient phase, it settles down to an stationary value within a 2% difference with respect to the initial value, thus making clear the ability of the code to keep the torus in equilibrium for the full evolution. In addition, the evolution of the central rest-mass density of the perturbed model (A1.2p) shows clearly that the initial perturbation induce a persistent phase of oscillations around the equilibrium position marked by the unperturbed model.

Results from a representative model with higher magnetic field are shown in the right panel of Fig. 1

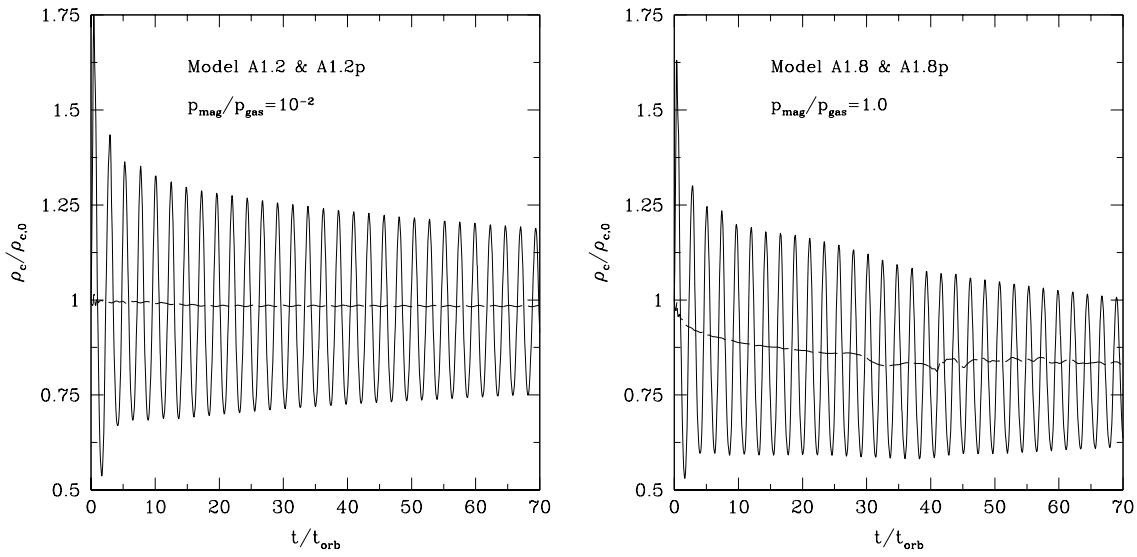

Figure 1. Time evolution of the central rest-mass density normalized to its initial value for models A1.2 (left panel) and A1.8 (right panel). Both panels show evolutions for both the unperturbed (dashed lines) and the perturbed models (solid lines).

that plots the time evolution of the normalized central density for both perturbed and unperturbed model A1.8, with matched magnetic-to-gas pressure ratio at the centre (i.e., $\beta_c = 1$). Overall the dynamics is very similar to model A1.2p shown in the left panel, and the p-mode oscillations are persistent during the entire evolution, the oscillations showing almost no damping even when $\beta_c = 1$. It is important to note that for tori with $\beta_c > 1$ the initial solution degrades over time as a significant accretion flux is induced in these cases and increases with the strength of the magnetic field.

5.2. Power Spectrum

Through a Fourier analysis of the time evolution of the hydrodynamic variables it is possible to obtain further information on the quasi-periodic behavior of the tori. For this purpose we Fourier transform the time evolution of the L_2 norm of the rest-mass density for all models, defined as $||\rho||^2 \equiv \sum_{i=1}^{N_r} \sum_{j=1}^{N_\theta} \rho_{ij}^2$. An important feature of axisymmetric p-mode oscillations of tori is that the lowest-order eigenfrequencies appear in a sequence $2:3$. This feature was first discovered in the nonlinear purely hydrodynamical numerical simulations of Zanotti et al. [7] and subsequently confirmed through a perturbative analysis in a Schwarzschild spacetime (Rezzolla et al. [16]) which was later extended to a Kerr spacetime and more general distributions of the specific angular momentum by Zanotti et al. [17] and Montero et al. [18]. Overall, it was found that the $2:3$ harmonic sequence was present with a good accuracy, within 10% error for tori with a constant distribution of specific angular momentum and within 20% error for tori with a power law distribution of angular momentum. Since the $2:3$ harmonic sequence is the result of the global mode of oscillation, it depends on a number of different elements that contribute to those deviations from an exact relation among the integers. In particular, the size of the disc, the location of the rest-mass density maximum, the black hole spin, the distribution of specific angular momentum, or the equation of state considered, can all influence this departure.

In Fig. 2 we plot the power spectrum obtained from the L_2 norm of the rest-mass density for models

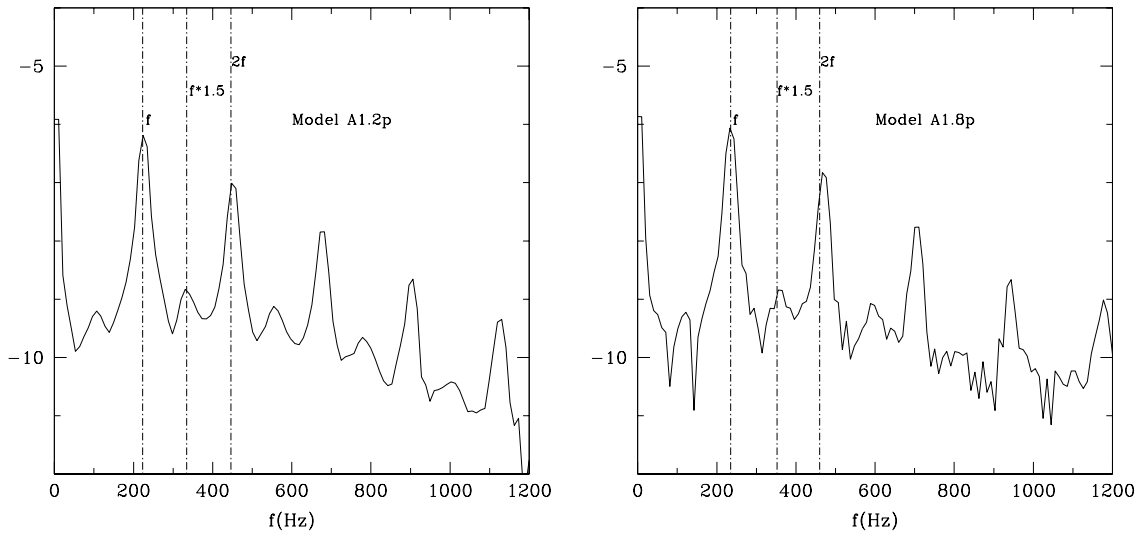

Figure 2. Power spectrum of the L-2 norm of the rest-mass density evolution for models A1.2p (left panel) and A1.8p (right panel).

A1.2p and A1.8p. In the left panel of this figure we show the power spectrum of model A1.2p while the right panel displays the one computed for model A1.8p; we also show three dashed vertical lines at the frequency of the fundamental mode, at $1.5f$ and at $2f$. A first result that emerges from the Fourier analysis is that the overall dynamics of magnetized tori with constant angular momentum shows similar features to those found by Zanotti et al. [7,17] for unmagnetized accretion tori around black holes. Namely, the spectra show a fundamental mode f and a series of overtones, where in particular the first overtone o_1 can be identified clearly. One of the most important features of the p-modes oscillations found in relativistic tori was that the first overtone and the fundamental mode appear in a harmonic sequence of $3:2$ to a very good accuracy. Our GRMHD simulations show that this is also valid for oscillations of magnetized tori where the o_1/f ratio is close to $3/2$. We report in Table 2 the frequency of the fundamental mode, the first overtone and their o_1/f ratio for four representative models of our sample with varying strength for the magnetic field. The figures reported reflect that there is a small shift in the peaks of the f and $o1$ modes toward higher frequencies as we increase the strength of the magnetic field, but however the o_1/f ratio is kept close to $3/2$ to a good accuracy. Thus, it seems that for magnetized torus the effect of a tororidal magnetic field on the p-mode oscillations is not very significant.

Among the several models proposed for the HFQPOs observed in LMXBs containing a black hole candidate, the one suggested by Rezzolla et al. [19] is based on the assumption that the accretion disc around the black hole terminates with a sub-Keplerian part, *i.e* a torus of small size. A key point of this model is the evidence, both numerical and analytic, that in these objects the fundamental mode and the first overtone are found to be in the $2:3$ harmonic sequence to a good precision and in a very wide parameter space. As shown by the simulations of magnetized tori presented here, it is clear that this $2:3$ harmonic sequence is also present in magnetized tori with a good precision, which confirms the validity of this model of HFQPOs based on quasi-periodic oscillations of tori in a more general context where the toroidal magnetic field structure of the torus is taken into account.

As mentioned briefly above, another important feature in the disc dynamics is the presence of

Table 2. From left to right, the columns report the name of the model, the frequency of the fundamental mode, the frequency of the first overtone, their ratio, and the magnetic-to-gas pressure ratio at the centre of the torus.

Model	f (Hz)	o_1 (Hz)	o_1/f	(β_c)
A1.1	224	332	1.48	0.00
A1.2	224	332	1.48	0.01
A1.6	229	338	1.47	0.20
A1.8	235	341	1.45	1.00

nonlinear couplings between oscillation modes. This feature of the p-mode oscillations of relativistic tori was first pointed out in Zanotti et al. [17] in their investigation of the dynamics of purely hydrodynamical tori with nonconstant specific angular momentum in Kerr spacetime. Such nonlinear harmonics, consequence of the nonlinear coupling among modes, appear in particular as combinations of f and o_1. Thus, from the spectra in Fig. 2, the peak at $2f$ can be interpreted as a result of this coupling effect. We note that the presence of the nonlinear harmonics is insensitive to the values of the parameter β_c considered in those models and that the peak at $2f$ could be readily identified even in the model with $\beta_c = 1$.

6. Conclusions

We have studied the dynamics of magnetized relativistic axisymmetric tori orbiting in the background spacetime of a Schwarzschild black hole. The tori are modeled as having a purely toroidal magnetic field and a constant distribution of the specific angular momentum. We have neglected the self-gravity of the disc and the accretion of mass and angular momentum has been assumed not to affect the Schwarzschild background metric. The results presented in this paper have extended previous investigations of tori in a purely hydrodynamical context (Zanotti et al. [7,17]).

Overall, we have found that the dynamics of the magnetized tori considered here is very similar to that found in the purely hydrodynamical case by Zanotti et al. [7,17]: The introduction of a perturbation, for the values of the magnetic field considered here, triggers quasi-periodic oscillations lasting tens of orbital periods. As in the hydrodynamical case, the spectral distribution of the eigenfrequencies showed the presence of a fundamental p-mode and of overtones in a harmonic ratio: $2 : 3 : \ldots$. We found that there was a small shift in the peaks of the fundamental and first overtone modes towards higher frequencies as we increased the strength for the magnetic field. In addition, nonlinear harmonics, consequence of the nonlinear coupling among modes, appeared in particular, as combinations of f and o_1.

The simulations of magnetized tori presented here confirmed the validity of the model of HFQPOs proposed by Rezzolla et al. [19], based on quasi-periodic oscillations of tori, in a more general context where the toroidal magnetic field structure of the torus is taken into account.

Acknowledgments

This research has been supported by the Spanish Ministerio de Educación y Ciencia (grant AYA2004-08067-C03-01). P.M. is supported by a VESF Postdoctoral Fellowship grant (EGO-DIR-126-2005). The Computations were performed on the computer "CERCA2" (42 CPUs Opteron dual core,92 GB) of the Department of Astronomy and Astrophysics of the University of Valencia.

References

[1] Balbus S A and Hawley J F 1991 *ApJ* **376** 214
[2] Blandford R D and Znajek R L 1977 *MNRAS* **179** 433

[3] De Villiers J and Hawley J F 2003 *ApJ* **589** 458
[4] Gammie C F, McKinney J C and Toth G 2003 *ApJ* **589** 444
[5] Antón L, Zanotti O, Miralles J A, Martí J M, Ibáñez J M, Font J A and Pons J A 2006 *ApJ* **637** 296
[6] Komissarov S S 2006 *MNRAS* **368** 993
[7] Zanotti O, Rezzolla L and Font J A 2003 *MNRAS* **341** 832
[8] Kozlowski M, Jaroszynski M, Abramowicz M A 1978 *A&A* **63** 209
[9] Abramowicz M A, Jaroszyński M and Sikora M 1978 *A&A* **63** 221.
[10] Font J A and Daigne F 2002 *MNRAS* **334** 383
[11] Shibata M, Taniguchi K, Uryū K 2003 *Phys. Rev. D* **68** 084020
[12] Shibata M, Taniguchi K, Uryū K 2005 *Phys. Rev. D* **71** 084021
[13] Michel F 1972, *Astrophys. Spa. Sci.* **15** 153
[14] Evans C and Hawley J F 1988 *ApJ* **207** 962
[15] Ryu D, Miniati F, Jones T W and Frank A 1998 *ApJ* **509** 244
[16] Rezzolla L, Yoshida S'i, Zanotti O 2003 *MNRAS* **344** 978
[17] Zanotti O, Font J A, Rezzolla L, Montero P J 2005 *MNRAS* **356** 1372
[18] Montero P J, Rezzolla L and Yoshida S'i 2004 *MNRAS* **354** 1040
[19] Rezzolla L, Yoshida S'i, Maccarone T J and Zanotti O 2003 *MNRAS* **344** L37